Research on a square Cassegrain-type solar concentrating reflector with a double pyramid

Yao Zhang, Huajun Yang*, Ping Jiang, Shengqian Mao, Mingyin Yu

School of Physical Electronic, University of Electronic Science and Technology of China, Chengdu 610054, China

*Corresponding author: yanghj@uestc.edu.cn

A structure of a solar concentrating reflector is designed in this paper to improve the usage of solar energy. For the dark image which is the result of the secondary mirror in the new type of the Cassegrain solar concentrating system, a double pyramid system is used to improve this phenomenon. By eliminating the dark image, the system enhanced the concentration ratio and the working efficiency. Meanwhile, both the primary and secondary mirrors are shaped into a square section in order to get a better match with a square photovoltaic receiver. While the length of the primary mirror is 89 m and the block ratio is 20%, the concentration ratio is equal to 118.86.

Keywords: concentrating reflector, double pyramidal, ray tracing.

1. Introduction

With the rapid development of industry, the usage of new energy resources becomes more and more important, and it has attracted many researchers' attention in the past forty years. Among the existing new energy sources, solar energy has attracted more interest than other because of its advantages such as abundant, inexhaustible, free, widely spread. And therefore the study of a solar concentrating reflector is of a great value in improving the efficiency of solar system [1–4].

In recent decades, innovative structures of the solar concentrating reflector have been proposed. The reflector comprises two mirrors: primary and secondary [5]. Generally, the primary mirror is designed as a parabolic surface, and the design of the secondary has many options. This structure greatly improves the concentration ratio and thus possesses an obvious advantage over refractive lens concentrators in the capability of concentrating [6]. Among these options put forward by researchers, Cassegrain reflectors have attracted more attention due to their good performance. With the wide spread use of it, its shortcomings are gradually being discovered, and attract attention of many researchers, who try to eliminate them [7–10]. When light is reflected by the

secondary mirror, a dark image can be generated on the photovoltaic (PV) receiver because of the imaging characteristics. This means the PV receiver cannot receive light uniformly and reduces the service life of the solar concentration system [11, 12]. Research on this phenomenon is necessary. Also, since the emerging light shape is a circle, different from the shape of the PV receiver, a waste exists and the light received is not uniform as well. Shaping light into a square beam is important to enhance the utilization of the PV receiver [13, 14].

In this study, a new type of solar concentrating optical system is proposed to eliminate the dark image caused by the secondary mirror based on the Cassegrain concentrating reflector structure. A new method is also put forward to obtain square-shape emerging light to enhance utilization efficiency of the square PV receiver. The work is based on ray tracing, and a mathematical model is built through some amount of derivation and calculation. Finally, the accuracy is verified by simulation using MATLAB.

2. Design of the solar concentrating reflector

The structure of the Cassegrain solar concentration system is shown in Fig. 1. Assume that the incident sunlight is parallel, as it is shown in Fig. 1, and the primary mirror of the general Cassegrain solar concentration system reflects the incident sunlight on the secondary mirror, then the secondary mirror will reflect the light in parallel because of the same focal point they have while the incident sunlight is parallel. Then the dark image will be generated which is shown in the picture. Generally, there is a divergence of ±0.27°, which will influence the emerging ray as well. And the circle beam cannot achieve the best utilization of the PV receiver. In order to eliminate the dark area and get square beam, we do some improvements on the structure. In this paper, the surfaces
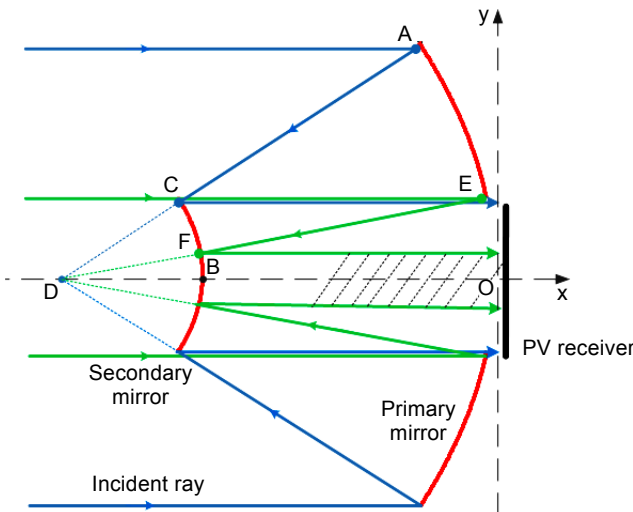

Fig. 1. Structure of Cassegrain-type solar concentration system.

for both the primary mirror and the secondary mirror of the system are designed as a one-dimensional photonic crystal structure, which is made of SiO_2 and TiO_2 media. The thicknesses of SiO_2 and TiO_2 are 0.1714 and 0.0878 µm, respectively, and the total reflection wavelength range is 0.3611 to 1.660 µm, which can reach a high total reflection in the range from visible light to near infrared wavelength [15].

2.1. Generating the hollow square beam

In this paper, we get a square beam by using a square aperture mirror, and both of them are parabolic mirrors because of their advantages such as eliminating the spherical aberration and simple calculation. The two-dimensional practical structure diagram is shown in Fig. 1, similar to the traditional one. Both of the reflectors are formed by rotating the generatrix around the symmetry x-axis, which is toward the sun. The equations of the primary mirror can be expressed as

$$y_1^2 = -2px_1 \tag{1}$$

where p is the distance between the focal point $D(-0.5p, 0)$ and the alignment.

Suppose the coordinates of point $A(-0.5l^2/p, l)$ and point $B(-l_1, 0)$, where $2l$ and l_1 represent the length of the primary mirror and the distance between the central point of the secondary mirror and the primary mirror.

As the secondary mirror shares the same focal point $D(-0.5p, 0)$ with the primary mirror, we have the two-dimensional curve equation of the secondary mirror as

$$y_2^2 = -4\left(\frac{p}{2} - l_1\right)(x_2 + l_1) \tag{2}$$

According to the geometrical knowledge, we know that the line AC (see Fig. 1) satisfying

$$y_{AC} = \frac{2pl}{p^2 - l^2}\left(x + \frac{p}{2}\right) \tag{3}$$

By Equations (2) and (3) we get that

$$y_C = \frac{l(p - 2l_1)}{p} \tag{4}$$

which is the y-axis coordinate of point C, and also the half of the length of the secondary mirror. Then we have the block ratio N

$$N = \frac{y_C^2}{l^2} = \frac{(p - 2l_1)^2}{p^2} \tag{5}$$
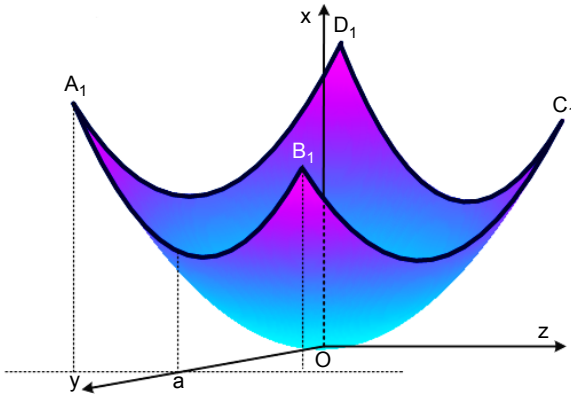
Fig. 2. Square cross-section of a rotating parabolic reflector.

From Eq. (5), the positions of the two mirrors can be determined when the block ratio N is known. Similarly, the x-axis coordinate of point F can be obtained

$$y_F = \frac{l(p - 2l_1)^2}{p^2} = \frac{p - 2l_1}{p} y_C \qquad (6)$$

which is half of the length of the hollow beam. Equation (6) shows that while the values of p and l_1 are fixed, the length of the hollow beam varies directly as the length of the secondary mirror. Figure 2 is the three-dimensional structure diagram of the reflectors with a square cross-section, which is a rotated symmetrical about x-axis, and the three -dimensional equation can be expressed as $x = 0.5(y^2 + z^2)/p$.

In Figure 2, A_1, B_1, C_1 and D_1 are the points of the inscribed square of the aperture of the reflector. Assume the diameter is $2\sqrt{2}a$, and then a is the distance between the edge of the cross-section and the origin point O (0, 0). So the curves can be expressed as

$$\stackrel{\frown}{A_1B_1}: \quad x = 2p(a^2 + y^2) \quad \text{for} \quad -a < y < a, \quad x = a \qquad (7a)$$

$$\stackrel{\frown}{B_1C_1}: \quad x = 2p(z^2 + a^2) \quad \text{for} \quad -a < x < a, \quad y = a \qquad (7b)$$

$$\stackrel{\frown}{C_1D_1}: \quad x = 2p(a^2 + y^2) \quad \text{for} \quad -a < y < a, \quad x = -a \qquad (7c)$$

$$\stackrel{\frown}{D_1A_1}: \quad x = 2p(z^2 + a^2) \quad \text{for} \quad -a < x < a, \quad y = -a \qquad (7d)$$

By the above equations we can get the square cross-section easily, which is more convenient for lining the reflectors in array.

The simulations of a solar concentration system based on the calculations above are shown in Fig. 3.

Figure 3**a** is the ray tracing of a solar concentration reflector in a square cross-section. Figures 3**b** and 3**c** present the emerging light in the condition of parallel incident light and incident light with the divergence of 0.27°, respectively. From Fig. 3 we can
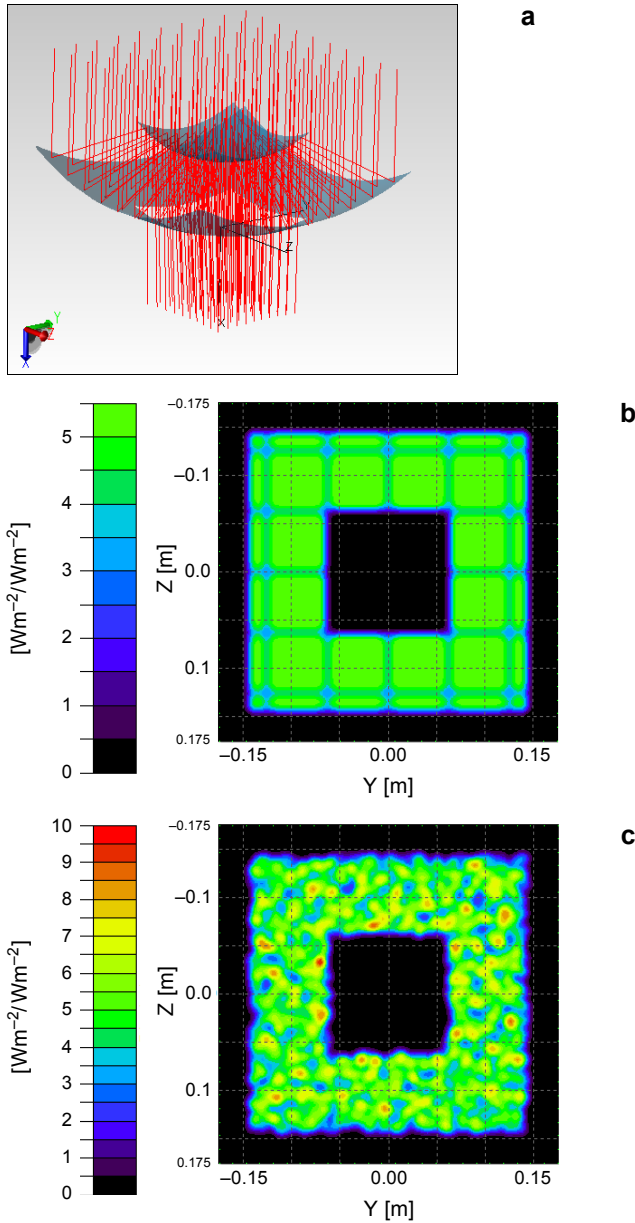
Fig. 3. Simulation of the solar concentration system (see text for explanation).

see that light passing through the solar concentration reflector in Fig. 3**a** is shaped into a square hollow beam with uniform distribution, which is shown in Fig. 3**b**. Figure 3**c** shows that while there is a divergence of 0.27°, the uniformity is a little lower than the condition of parallel incident light and the shape is a little irregular than the former condition.

2.2. Transform hollow beam into solid beam

As is known from the characteristics of the pyramid, light shot on the pyramid vertical to its bottom will have a beam splitting due to the refraction. Then, the two beams of light which are central axis-symmetric for the pyramid will be combined into one beam because of the optical reversibility. In order to obtain parallel emerging light in the direction same with incident light, we put another pyramid under the first one, making their bottoms coincide perfectly. In this paper, the double pyramid is put above the PV receiver to get the solid beam, and is made of K9 glass ($n = 1.51$) which is coated with multispectral antireflection coatings [16].

The structure of the solar concentration system with a double pyramid is shown in Fig. 4. The annular beam generated by the reflection of the secondary mirror falls on the double pyramid system, changes into a solid one and is received by the PV receiver. Figure 5 shows the trace of light passing through the double pyramid system in two-dimensions. In Fig. 5, the double pyramid system is shown as a side view.
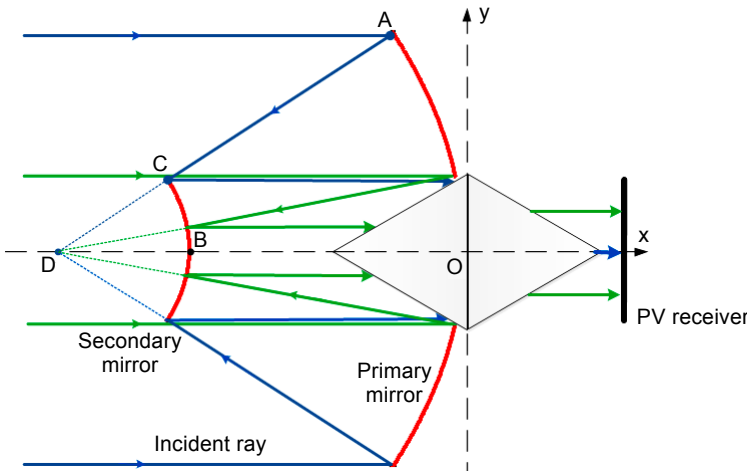

Fig. 4. Structure of the solar concentration system with a double pyramid.
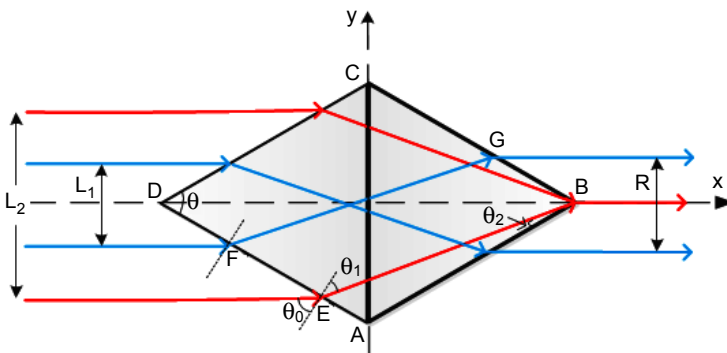

Fig. 5. Trace of light passing through a double pyramid system.

As the coordinate shown in Fig. 5, $A(0, -h\tan(0.5\theta))$, $B(h, 0)$, $C(0, h\tan(0.5\theta))$, and $D(-h, 0)$ are the vertices of a double pyramid, which h and θ are the height and dip angle of one of the pyramids, respectively. So the expression of line EB is

$$y = -x\tan(0.5\theta) - h\tan(0.5\theta) \tag{8}$$

The edge of the beam crosses the surface of the pyramid at point E. The y-axis of E is $-0.5L_2$ (L_2 is the width of the hollow beam), and by Eq. (8) we can get the coordinate of point $E([L_2/(2\tan(0.5\theta) - h], -0.5L_2)$. The slop k_1 of line EB is

$$k_1 = \frac{L_2\tan(0.5\theta)}{4h\tan(0.5\theta) - L_2} \tag{9}$$

In Figure 5, θ_0 and θ_1 are the incident angle and refraction angle, respectively. By geometry $\theta_2 = \theta_0 - \theta_1 = 0.5\pi - 0.5\theta - \theta_1$. Therefore, k_1 also can be expressed as

$$k_1 = \tan(\theta_2) = \frac{\cot(0.5\theta) - \tan(\theta_1)}{1 + \cot(0.5\theta)\tan(\theta_1)} \tag{10}$$

Based on the law of refraction,

$$\tan(\theta_1) = \frac{\dfrac{n_0}{n_1}\cos(0.5\theta)}{\sqrt{1 - \left[\dfrac{n_0}{n_1}\cos(0.5\theta)\right]^2}} \tag{11}$$

where n_0 and n_1 represent the refractive indexes of air and the material of the pyramid. Substituting Eq. (11) into Eq. (10), we can get

$$k_1 = \frac{\sqrt{1 - \left[\dfrac{n_0}{n_1}\cos(0.5\theta)\right]^2}\cos(0.5\theta) - \dfrac{n_0}{n_1}\cos(0.5\theta)\sin(0.5\theta)}{\dfrac{n_0}{n_1}\cos^2(0.5\theta) + \sin(0.5\theta)\sqrt{1 - \left[\dfrac{n_0}{n_1}\cos(0.5\theta)\right]^2}} \tag{12}$$

By Eqs. (9) and (12) the relationship between L_2 and θ is

$$L_2 = \frac{2h\sin(\theta)\left\{\sqrt{1 - \left[\dfrac{n_0}{n_1}\cos(0.5\theta)\right]^2} - \dfrac{n_0}{n_1}\sin(0.5\theta)\right\}}{\sqrt{1 - \left[\dfrac{n_0}{n_1}\cos(0.5\theta)\right]^2}} \tag{13}$$
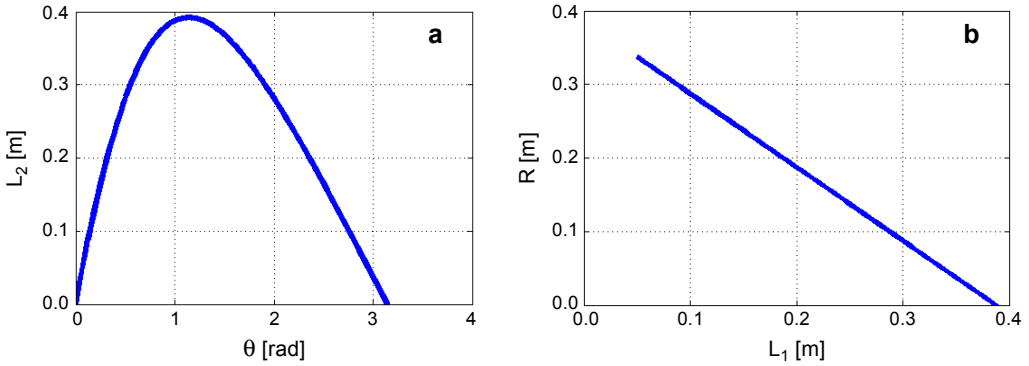
Fig. 6. Results of calculation (see text for explanation).

The curve in Fig. 6**a** shows the relationship between L_2 and θ, and the pyramid can be determined when L_2 is known. Because the equations of line AD and line CB are

$$y_{AD} = -x\tan(0.5\theta) - h\tan(0.5\theta) \tag{14a}$$

$$y_{CB} = -x\tan(0.5\theta) + h\tan(0.5\theta) \tag{14b}$$

and the y-axis of point F and G are known, the x-axis of them can be got. Then we have the slop of line FG

$$k_{FG} = \frac{(R + L_1)\tan(0.5\theta)}{4h\tan(0.5\theta) - (R + L_1)} \tag{15}$$

where L_1 and R are the width of the internal hollow of the beam and the width of the solid beam emerged, respectively. Line FG is parallel with line EB, thus, $k_{FG} = k_1$. By Eqs. (12) and (15), we have the relationship between R and L_1

$$R = 2h\sin(\theta) - \frac{2\dfrac{n_0}{n_1}h\sin(\theta)\sin(0.5\theta)}{\sqrt{1 - \left[\dfrac{n_0}{n_1}\cos(0.5\theta)\right]^2}} - L_1 \tag{16}$$

which is shown in Fig. 6**b**.

Figure 6**a** is the relationship between the dip angle of the pyramid θ and the width of the hollow beam L_2, and Fig. 6**b** is the relationship between the width of the internal hollow L_1 and the width of the emerging beam R. In Fig. 6**a**, we set $h = 0.37$ m and from the relationship which is shown in the picture we can see that the width of the hollow beam L_2 is firstly ascended and then descended with the increase of the dip angle of the pyramid θ, and achieves the peak at 1.241 rad (71.082°). Therefore, $\theta = 0.991$ rad (56.786°) is chosen in Eq. (16) in order to avoid the total reflection of the pyramid, and, similarly, $h = 0.37$ m. As it is shown in Fig. 6**b**, the width of the emerging beam R

is decreased with the rise in the width of the internal hollow L_1. The concentration ratio (CR) is

$$\text{CR} = \frac{4l^2(1-N)}{R^2} = \frac{4l^2(p-2l_1)^2}{\left\{ p\sqrt{1 - \left[\dfrac{n_0}{n_1}\cos(0.5\theta)\right]^2} - p + 2l_1 \right\}^2} \tag{17}$$
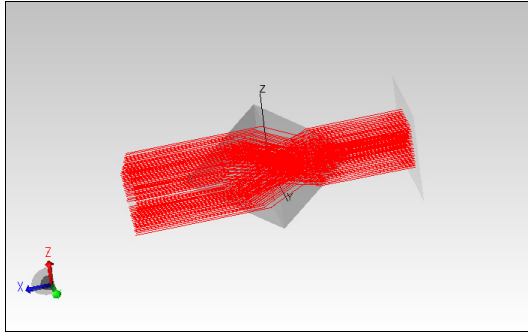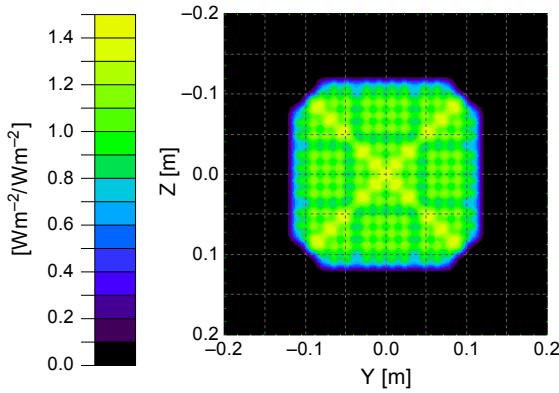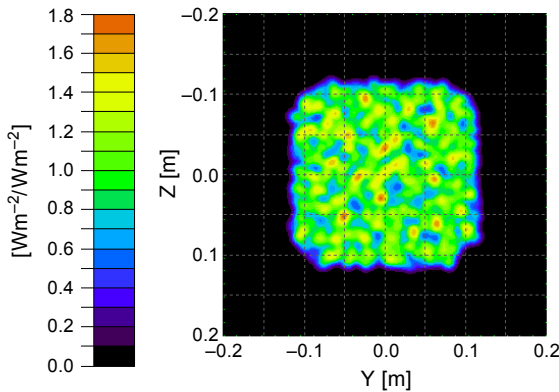
Fig. 7. Simulation of the double pyramid system (see text for explanation).

Assume the block ratio N is 20%, and set $l = 0.447$ m, according to Eqs. (5), (6), (13) and (17) the concentration ratio CR is 118.86. This high concentration mainly due to the elimination of the central shadow. And the uniformity, which is an important property of the solar concentration system, is also improved. The simulations of the double system in the conditions of parallel incident sunlight and incident sunlight with a divergence of 0.27° are shown in Fig. 7.

Figure 7**a** is the ray tracing of the double pyramid system, and Figs. 7**b** and 7**c** are the emerging ray in conditions of parallel incident sunlight and incident sunlight with a divergence of 0.27°, respectively. As it is shown in Fig. 7**a**, the double pyramid system transforms the hollow beam from the concentrating system into a solid beam (shown in Figs. 7**b** and 7**c**). It indicates that the uniformity is good while the incident sunlight is parallel from Fig. 7**b**. While there is a divergence of 0.27° of sunlight, the uniformity is lower than when it is parallel, and the shape of an emerging ray is also more irregular than it is parallel. The aim of this work has been achieved, the concentration ratio is increased.

3. Conclusions

This study designed a complete solar concentration system. Using the ray tracing and the mathematical method, the paper shows the way of generating square beams which improves the limitation of the traditional solar concentration system of a Cassegrain-type. As its square-cross-section, this kind of solar concentrating reflectors can be arranged in array easily. The dark image is eliminated and the concentration ratio is increased at the same time, which improves the utilization of a PV receiver effectively. The service life of the PV receiver is also enhanced due to the uniform incident light on it. Therefore, the cost of the concentration system is reduced. And while the length of the primary mirror 89 m and the block ratio is 20%, concentration ratio is equal to 118.86. Based on numerous calculations, the feasibility is proved by simulation.

References

[1] STEWARD W.G., KREITH F., *Stationary concentrating reflector cum tracking absorber solar energy collector: optical design characteristics*, Applied Optics **14**(7), 1975, pp. 1509–1512.
[2] GORDON J.M., *Aplanatic optics for solar concentration*, Optics Express **18**(S1), 2010, pp. A41–A52.
[3] ARAKI K., YANO T., KURODA Y., *30 kW concentrator photovoltaic system using dome-shaped Fresnel lenses*, Optics Express **18**(S1), 2010, pp. A53–A63.
[4] XING HUANG, YUAN YUAN, YONG SHUAI, BING-XI LI, HE-PING TAN, *Development of a multi-layer and multi-dish model for the multi-dish solar energy concentrator system*, Solar Energy **107**, 2014, pp. 617–627.

[5] GORDON J.M., FEUERMANN D., *Optical performance at the thermodynamic limit with tailored imaging designs*, Applied Optics **44**(12), 2005, pp. 2327–2331.

[6] GORDON J.M., *Recent developments in nonimaging secondary concentrators for linear receiver solar collectors*, Proceedings of SPIE **1528**, 1991, p. 32.

[7] ZHENG ZHOU, QIANG CHENG, PINGPING LI, HUAICHUN ZHOU, *Non-imaging concentrating reflectors designed for solar concentration systems*, Solar Energy **103**, 2014, pp. 494–501.

[8] QIANG CHENG, JIALE CHAI, ZHENG ZHOU, JINLIN SONG, YANG SU, *Tailored non-imaging secondary reflectors designed for solar concentration systems*, Solar Energy **110**, 2014, pp. 160–167.

[9] CHI-FENG CHEN, CHIH-HAO LIN, HUANG-TZUNG JAN, YUN-LING YANG, *Design of a solar concentrator combining paraboloidal and hyperbolic mirrors using ray tracing method*, Optics Communications **282**(3), 2009, pp. 360–366.

[10] WHANG J.W., BO-YI WU, YI-YUNG CHEN, *Innovative design of cassegrain solar concentrator system for indoor illumination utilizing chromatic aberration to filter out ultraviolet and infrared in sunlight*, Proceedings of SPIE **6896**, 2008, article 689619.

[11] JIN JING-SHEN, SHU BI-FEN, SHEN HUI, LI JUN-YONG, CHEN MEI-YUAN, *The temperature and illumination intensity characteristic of the monocrystalline silicon solar cell*, Material Research and Applications **2**(4), 2008, pp. 498–501.

[12] RADZIEMSKA E., *Performance analysis of a photovoltaic-thermal integrated system*, International Journal of Photoenergy, 2009, article 732093.

[13] KWANGSUN RYU, JIN-GEUN RHEE, KANG-MIN PARK, JEONG KIM, *Concept and design of modular Fresnel lenses for concentration solar PV system*, Solar Energy **80**(12), 2006, pp. 1580–1587.

[14] SHIH-HSIN MA, CHUN-MING TSENG, YUN-PARN LEE, *Generation of a uniform-square focal spot by a compound lens for solar concentration applications*, Applied Optics **52**(13), 2013, pp. 3058–3065.

[15] WEN-SHENG L.I., HUANG H.M., YAN-HUA F.U., ZHANG Q., SHI D.F., *Design of highly efficient reflector of solar cells based on photonic crystal*, Laser and Infrared **41**(8), 2011, pp. 885–888.

[16] SOKOLOVA R.S., MIKHAILOV A.V., MURANOVA G.A., GORELKINA Z.N., *Multispectral antireflection coatings for the visible, near-IR, and IR regions*, Journal of Optical Technology **72**(10), 2005, pp. 784–786.